Crystallization and Transient Mesophase Structure in Cold-Drawn PET Fibers

Jong Kahk Keum,[†] Jinmo Kim,[†] Sang Man Lee,[†] Hyun Hoon Song,*[,†] Yang-Kug Son,[‡] Jong-In Choi,[‡] and Seung Soon Im[§]

Department of Polymer Science and Engineering, Hannam University, Daejeon, S. Korea; R & D Center for Fiber and Textile, Hyosung Corporation, Anyang, S. Korea; and Department of Fiber and Polymer Engineering, Hanyang University, Seoul, S. Korea

Received May 26, 2003; Revised Manuscript Received October 1, 2003

ABSTRACT: Transient structure and crystallization behaviors in cold-drawn PET fibers were studied by synchrotron wide-angle X-ray diffraction, IR spectroscopy, and thermomechanical analysis. As-spun PET fibers were mechanically cold-drawn up to the breaking point, and those stretched ones beyond the strain hardening point in the stress−strain curve exhibited the transient layer structure. Evidence suggesting the tilted PET chains within the transient layer structure, and therefore the smectic C mesophase, was discussed. The tilt angle of the chains within the layer was 6° against the fiber axis. The tilt angle, however, decreased rapidly with the crystallization. Results of X-ray diffraction, IR absorbance, and thermomechanical analysis suggested two-stage crystallization in oriented PET chains. Bundles of highly oriented chains including the mesophase were responsible for the first stage crystallization (80−100 °C), but those of less ordered or nonoriented chains were for the second stage crystallization beyond 140 °C. The structural transformation from the transient mesophase to the triclinic crystal structure was interpreted by the chain sliding mechanism, leading to the tilted (001) planes against the fiber axis.

Introduction

Poly(ethylene terephthalate) (PET) has a high glass transition temperature and a slow crystallization rate, which enables one to make nearly amorphous PET and thus easy to control final morphology.[1−3] The usages of PET in fibers and films are indeed based on the mechanical orientation of supercooled PET and subsequent heat treatment.[4−6] Accordingly, the orientation-induced crystallization process of mechanically oriented PET samples and the morphology have been extensively studied.[7−14] One of the interesting features associated with the orientation-induced crystallization of oriented amorphous PET is that the polymer exhibits a transient structure prior to the final triclinic crystal structure formation. The initial observation of the transient structure in PET crystallization was made decades ago by Bonart[8] and later by Asano et al.[10] In recent years, more detailed studies on this issue have been conducted by several researchers utilizing the synchrotron X-ray source.[15−19] Even though the interpretations differ slightly from one to another, they seem to agree that the transient structure consists of layers with paracrystalline or mesophasic order. In most cases, this intermediate mesophase structure is formed by the mechanical drawing of PET. It has been suggested that this intermediate structure acts as a precursor for the crystal formation in oriented PET.[17−20] Murthy et al.,[14] on the other hand, suggested that even in nonoriented amorphous PET there are short-range orders corresponding to the two different interchain distances, which are the incipient crystalline orders in (010) and (100) crystallographic directions. Yeh and Geil[12,13] also pointed out that melt-quenched PET is composed of ball-like structure of paracrystalline order and the strain-induced crystallization is caused by the spacial rearrangement of the paracrystalline domains and internal perfection of the domains. In this work, structure evolution in cold-drawn amorphous PET fibers upon elevating temperature was investigated in detail by combining the synchrotron X-ray scattering and IR spectroscopy as well as thermomechanical analysis. We were particularly interested in the intermediate structure often found in cold-drawn PET fibers or films and the crystallization process of the oriented PET chains.

Experimental Section

Preparation of Samples. High-speed melt-spun (3200 m/min) amorphous poly(ethylene terephthalate) fibers obtained from Hyosung Corp. were mechanically stretched at different levels up to the breaking point (0−135%). The initial length of fiber bundle was 12 cm, and the strain rate was 0.83 min^{-1}. The fibers were subsequently relaxed for 24 h at room temperature while maintaining the fiber length constant. The fiber samples were prepared in a bundle type (∼1180 deniers) for the X-ray diffraction experiments and other characterizations. For the preparation of nonoriented quenched PET sample, a vacuum-dried (at 100 °C for 24 h) PET chip was melted at 275 °C for 5 min and subsequently quenched in an ice water. The dimension of the film was 5 mm in diameter and 1 mm in thickness. The intrinsic viscosity of a PET chip and spun fiber was 0.64 dL/g.

Measurements. Structure evolution in cold-drawn amorphous fibers upon elevating temperature was examined by the time-resolved wide-angle X-ray diffraction (WAXD) utilizing a synchrotron X-ray source (2.5 GeV, 150 mA) at the 4C1 X-ray beamline in Pohang Accelerator Laboratory (PAL). The wavelength was 1.6083 Å, and the collimated beam size at the sample was 0.3 mm × 0.3 mm. Two-dimensional WAXD patterns were collected using a position-sensitive CCD detector with a spatial resolution of 100 μm × 100 μm. Exposure time for each pattern was 23 s. The sample-to-detector distance was calibrated with the benzoic acid crystal. FT-IR spectroscopy (Perkin-Elmer, 1000PC) was also utilized to study the confor-

[†] Hannam University.
[‡] Hyosung Corporation.
[§] Hanyang University.
* To whom correspondence should be addressed: telephone 82-42-629-7504, Fax 82-42-626-8841, e-mail songhh@mail.hannam.ac.kr.

10.1021/ma034694i CCC: $25.00 © 2003 American Chemical Society
Published on Web 12/06/2003

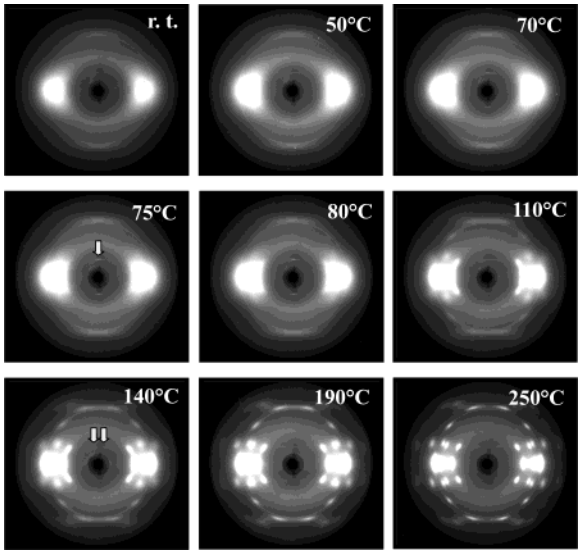

Figure 1. Selected wide-angle X-ray diffraction patterns of PET fiber measured at the corresponding temperatures upon heat treatment. The fiber was originally spun at 3200 m/min and subsequently cold-drawn by 120%.

mational changes of chains during crystallization. The scan interval was 1 cm^{-1}, and the heating rate was 3 °C/min. Modulated differential scanning calorimetry (MDSC) was used to examine the thermal behaviors such as glass transition temperatures and cold-crystallization temperatures of fibers. All experiments (WAXD, MDSC, FT-IR) were performed while maintaining the fiber length constant during the heat treatment. The contractive force emerging in the fiber upon elevating temperature was monitored by using a stress−strain tester (Shimatzu, AG-5000G) attached with a heating device.

Results and Discussion

Transient Mesophase Structure and Structure Evolution. Selected two-dimensional wide-angle X-ray diffraction (WAXD) patterns of PET fiber (spun at 3200 m/min and subsequently cold-drawn by 120%) measured at different temperatures are shown in Figure 1. The initial diffused diffraction pattern along the equator exhibits well-oriented but noncrystalline structure. As temperature increases, the patterns begin to show highly crystalline order, indicating typical triclinic crystalline structure development. One interesting feature, however, found in this series of diffraction patterns is the appearance of weak but sharp diffraction patterns at $2\theta = \sim 8.8°$ in the meridian. To examine the appearance of the meridional peak in detail, the meridional and equatorial slices derived from the two-dimensional patterns are plotted in parts a and b of Figure 2, respectively. The meridional slice (Figure 2a) reveals that the extremely weak but discernible reflection is noted even at room temperature, implying that the structural units responsible for the meridional reflection already exist in mechanically oriented chains before the thermal incitation. The transversely diffused meridional reflection (see Figure 1) begins to intensify when the temperature reaches ∼50 °C and maximizes at near 75 °C (arrow in Figure 2a), yielding an ordinary diffraction spot. Increasing the temperature further, however, the intensity becomes weak and transversely diffused again and finally splits into a four-point pattern. The new four-point reflection at off-axis stabilizes at 140 °C (see arrows in Figure 2c) and maintains the pattern on further increase of temperature, which assumed to be an (001) reflection of triclinic structure. The initial two-point meridional diffraction peak, on the other hand, can be associated with the transient structure prior to the triclinic crystal lattice formation, as proposed by a number of workers.[7−11,18,19] Because this transient meridional maximum has the spacing of ∼10.4 Å, nearly matching the monomer unit length (10.75 Å) of poly(ethylene terephthalate), we may regard this transient peak as $(001)_{trs}$. Here subscript "trs" denotes transient structure. The peak location and profile along the meridian and the layer line (Figure 2a,c) suggest that the diffraction is from the ordering of the chemical repeating units both in the direction of fiber axis and in the transverse direction across the chain bundles, where individual assembly of the repeat units across the chain bundles resembles a layered structure with the horizontal surface. The equatorial slice (Figure 2b) reveals that the chains within the layer maintain

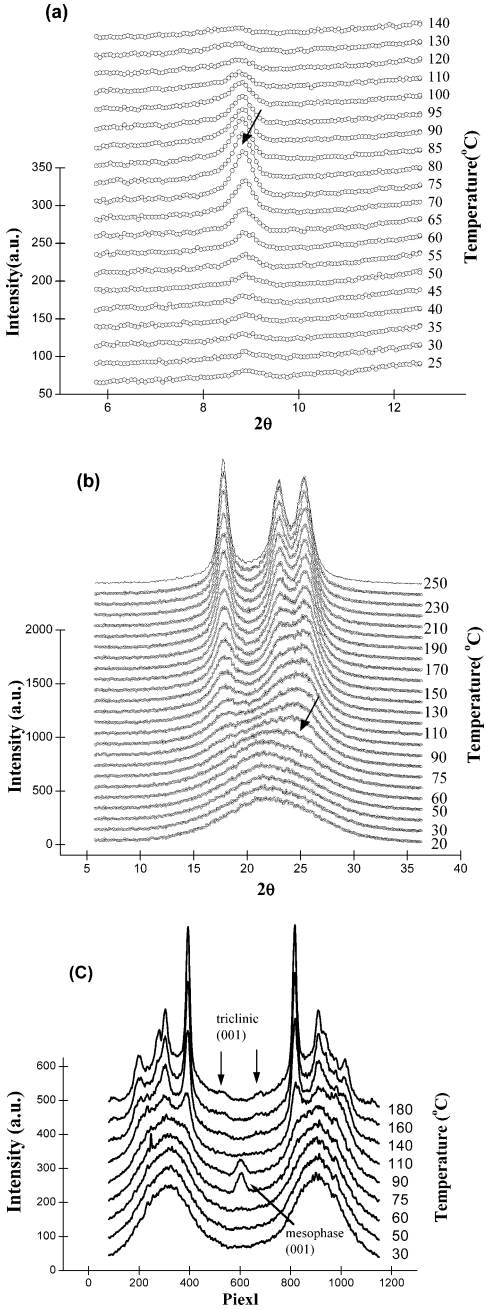

Figure 2. Meridional (a) and equatorial (b) slices and intensity profiles at (001) layer (c) obtained from the X-ray patterns shown in Figure 1.

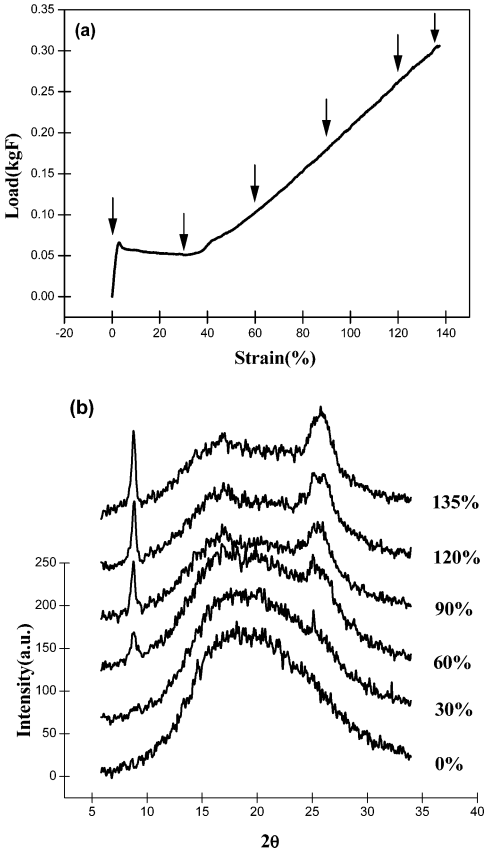

Figure 3. (a) Load−strain curve of the as-spun fiber and (b) meridional X-ray patterns of the cold-drawn fibers. The arrows and the numbers shown in the figure indicate the strain level where the X-ray diffraction was taken.

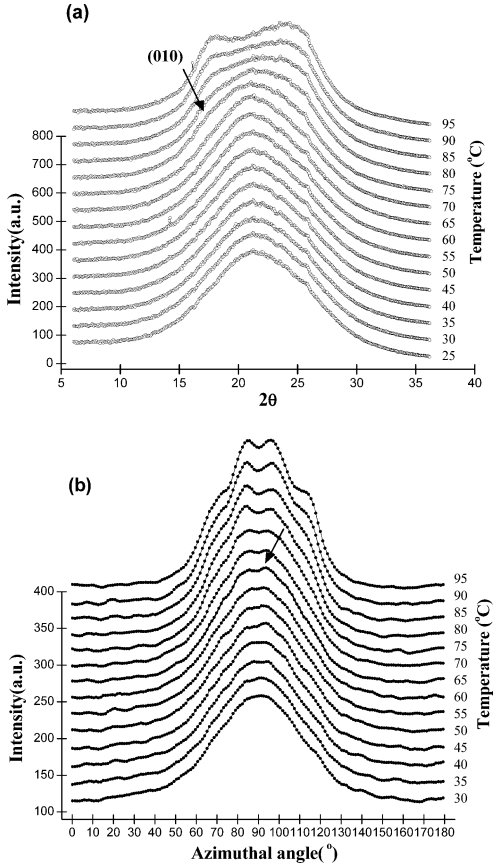

Figure 4. (a) X-ray intensity profiles along the 6° off-axis from the equator, where (010) reflection locates. (b) Azimuthal intensity distribution of (010) reflection at $2\theta = 17.8°$. The curves in (a) and (b) are obtained from the X-ray diffraction patterns shown in Figure 1.

amorphous state up to 75 °C. We also point out that the layer spacing of ~10.4 Å is somewhat shorter than the fully extended monomer length of 10.75 Å. The result implies that the chains within the layer are either tilted against the fiber axis or nonextended chain conformation.

Load−strain curve of high-speed melt spun PET (3200 m/min) fiber is plotted in Figure 3a. The arrows in the load−strain curve represent the stain levels where the stretched fiber was examined by the X-ray diffraction. Corresponding meridional intensity profiles of the fibers stretched and subsequently heat-treated at 75 °C are then plotted in Figure 3b. We emphasize that the $(001)_{trs}$ reflection is observed only in the fibers stretched beyond the strain hardening region. The peak intensifies with the increase of strain, but the peak position shown in Figure 3b remains unchanged. In polymer mechanics the strain hardening is associated with the formation of local-densified bundles of parallel-oriented chains.[21,22] This highly strained bundles of parallel chains must be responsible for the transient layer structure, and in order to accommodate further strain after the strain hardening, new chain elements are brought to their yield point to join the bundles and thus to intensify the $(001)_{trs}$ reflection. The constant layer spacing observed in the fibers of different levels of strain also implies that the chains in the densified bundle elements are nearly extended. The layer spacing that is somewhat shorter than the chemical repeat distance of PET, therefore, suggests tilted chains within layers.

Figure 4a shows the diffraction profiles along the off-axis (6° up or down the equator) obtained from the diffraction patterns shown in Figure 1. Also, curves in Figure 4b represent the azimuthal intensity profiles at $2\theta = 17.8°$, which corresponds to the (010) diffraction angle of the triclinic crystal of PET. The intensity profiles plotted in Figure 4a reveal that the (010) crystalline reflection becomes discernible at 75 °C, as was observed in the equatorial intensity profiles (Figure 2b), confirming the onset temperature of crystallization. We also note that its azimuthal profile (at $2\theta = 17.8°$) has double maxima, which can be noted even at temperatures below 75 °C (see arrow in Figure 4b). Observation of double maxima in azimuthal intensity distribution before reaching the crystallization temperature is a direct evidence to support that the chains within the transient layer structure are tilted against the fiber axis. Tilt angles of the *c*-axis derived from the double maxima of azimuthal distribution shown in Figure 4b are plotted in Figure 5. The curve shows that the chain tilt angle is about 6° and remains nearly constant until the temperature reaches about 80 °C. However, a drastic decrease of tilt angle is noted between 80 and 120 °C, where the crystallization takes place. As discussed in the previous section, a number of research results on the transient structure and the crystallization from the transient structure have been reported.[11−19] They agree that cold-drawn PET chains possess a transient paracrystalline or mesophase type order before the triclinic crystal structure formation. The tilted chain morphology in the transient structure was first discussed by Asano and Seto[10] in terms of the monoclinic structure. Very recently, Ran et al.[19] also suggested the

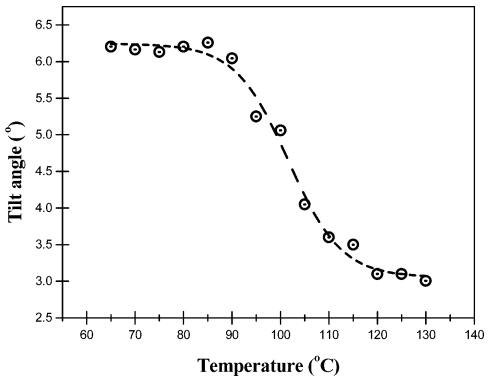

Figure 5. Chain tilt angles estimated from the azimuthal intensity distribution of (010) reflection at the indicated temperatures.

tilted chains in the mesophase based on the short layer spacing. Our experimental results also clearly demonstrate that the transient structure found in the oriented PET fiber is a smectic C type mesophase, where the chains within the layer are slightly tilted against the fiber axis. However, the tilt angles (Figure 5) estimated from the azimuthal split of scattered intensities at the (010) location are not sufficient to compensate the short layer spacing, suggesting that the chains may possess the conformational disorder as Auriemma et al.[23] suggested. This mesophase appears to be a frozen-in metastable state, induced by the mechanical drawing. When sufficient thermal motion is provided at the glass transition temperature, the metastable structure transforms into an equilibrium triclinic structure.

We recall that the maximized meridional peak becomes diffused again when the temperature is raised above 75 °C and the two-point pattern splits into four-point triclinic (001) reflection at 140 °C. The off-axis (001) peak illustrates that the initial horizontal layer surface becomes tilted against the fiber axis, and the tilt angle of the layer surface is about 60° against the fiber axis. The diffusion of diffraction peak implies a substantial rearrangement of the chains during this temperature interval. In Figure 6, suggested structures and corresponding meridional X-ray diffraction patterns are illustrated. The initial weak and transversely diffused pattern of $(001)_{trs}$ and equatorial amorphous halo below 50 °C suggests a broad distribution of layer orientation and lack of long-range order within the layer. The layer orientation and interlayer order gradually increase with the temperature and reach a maximum at 75 °C. In this temperature interval, the scale of chain rearrangement is probably only minimal at the local scale, and the chains within layer are still amorphous. Diffusion of diffraction spot noted above 75 °C suggests disordering of the layers, which is evidently associated with the orientation-induced crystallization of the mesophase to form more stable triclinic structure. Through this process, two-point $(001)_{trs}$ reflection splits into a new four-point pattern, demonstrating the tilting of layer surface. We recall that the chain tilt angle in the layer rather reduces at this temperature range, manifesting that the chains in the layer are sliding up or down along the fiber axis to result in crystalline order and tilted layer surface. The results suggest that the structural transformation from the smectic C type mesophase to the triclinic crystalline structure is achieved by the chain sliding process, which contradicts the chain tilting mechanism proposed by Asano et al.[11] The chain sliding probably can be attributed to the interactions

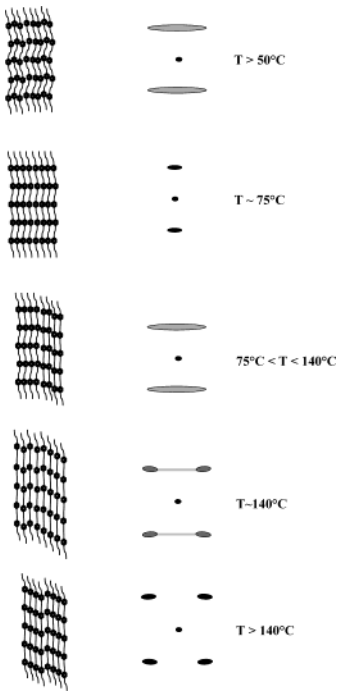

Figure 6. Suggested chain packing states and corresponding (001) X-ray diffraction patterns.

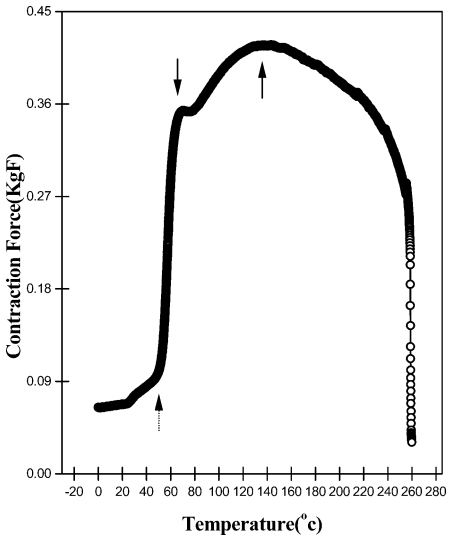

Figure 7. Plot of contractive forces emerging in the fiber upon heat treatment.

between adjacent phenylene rings and dipole−dipole interactions between adjacent carbonyl groups and ester groups.[7−10]

Two-Stage Crystallization of Oriented PET Chains. When oriented amorphous fiber is heat-treated, irreversible thermal deformation such as shrinkage or spontaneous elongation takes place. Thermal shrinkage is a well-known process that is associated with the entropic recovery of oriented chains. However, when the fiber length is held constant during the heat treatment, the force emerges in the fiber to compensate the thermal shrinkage. On the other hand, spontaneous elongation during heat treatment originates from the crystallization (gauche-to-trans conformational transformation).[24−28] In Figure 7, results of thermomechanical analysis of the PET fiber are plotted. The fiber originally spun at 3200 m/min was stretched further by 120%. The fiber was then held at constant length in an Instron, and the force

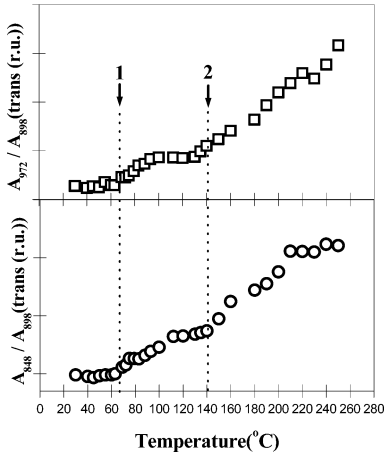

Figure 8. Ratio of IR absorption band of trans conformer at 845 and 972 cm^{-1} to that of gauche conformer at 898 cm^{-1}.

developing in the fiber was monitored during the temperature increase. As shown in the figure, the force imposed on fiber begins to increase drastically above 50 °C. When the temperature reaches about 70 °C, the load drops momentarily but continues to increase at a slower rate on further increase of temperature. The increase continues until the temperature reaches 140 °C. Beyond 140 °C, the load begins to decrease and shows a rapid drop as the temperature approaches the melting point. As discussed previously, the increase of load on fiber is related to the entropic recovery of oriented chains, while the decrease of the load is to the spontaneous elongation on crystallization. During heating scan of oriented amorphous fiber, the two opposing thermal deformations, shrinkage and elongation, shall progress competitively. When the recovery is dominant, the contractive force increases, but when the crystallization is dominant, it decreases. Recalling the X-ray diffraction results, the decrease of load noted at 70−80 °C and another decrease beyond 140 °C are evidently associated with the crystallization.

In an effort to investigate the crystallization process in greater detail, IR spectroscopy was also performed, and results are plotted in Figure 8.The characteristic absorption bands of the trans conformer are at 845 and 972 cm^{-1}, and that of gauche conformer is at 898 cm^{-1}.[29−32] These characteristic absorption bands correspond to the "wagging" of the oxyethylene group and to their trans and gauche conformations. The ratio (R) of trans conformer to gauche conformer can possibly indicate the relative amount of trans conformer in fiber (eq 1). [30]

$$R = \frac{A_{\text{trans}}}{A_{\text{gauche}}} \tag{1}$$

where A_{trans} is the infrared absorbance at 845 or 972 cm^{-1} and A_{gauche} is at 898 cm^{-1}. As depicted in Figure 8, we note a two-step increase of trans isomer content with the temperature increase. The ratio R begins to increase near 70 °C, and the increment levels off at 100 °C until another increase is observed beyond 140 °C. The result is consistent with those observed in the thermomechanical analysis, manifesting that the crystallization of oriented amorphous PET takes two crystallization processes. In an oriented supercooled amorphous fiber, the chain possesses a wide spectrum of chain orientation, from fully extended to poorly oriented

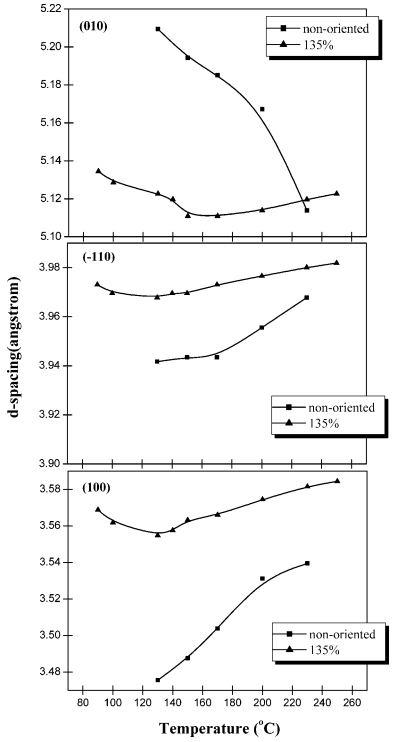

Figure 9. Comparison of d spacing changes of the crystal planes during crystallization process between highly oriented cold-drawn fiber and nonoriented sample.

chains. When the supercooled PET chains undergo crystallization upon raising temperature, the onset temperature of cold crystallization will differ depending on the chain orientation.[33] It is highly expected that the parallel-oriented chains in the mesophase crystallize first. Here we suggest that the crystallization noted between 70 and 100 °C is the first stage crystallization, primarily taking place in the mesophase, while the second stage crystallization noted beyond 140 °C is with the nonoriented or poorly oriented chains. Indeed, the cold crystallization of nonoriented amorphous PET exhibits an endothermic peak near 140 °C, while the oriented chains at much lower temperatures near the glass transition.

In Figure 9, d spacing changes of main reflections ((010), (−110), (100)) derived from the peak fitting using Gaussian line are depicted. It is interesting to observe that the d spacing of lateral crystal planes continues to decrease with temperature until the temperature reaches 140 °C. However, when the temperature is raised further above 140 °C, they begin to increase with the temperature. As we have suggested, the crystallization of the PET fiber follows the two-stage process, and 140 °C is the onset temperature of the second stage crystallization. It has been suggested that the unit cell for the equilibrium PET crystal may not be suitable for the fibers and films, each with their own characteristic strains.[34,35] A relationship between internal stress and unit cell parameters of PET fiber has also been proposed.[36] The decrease of d spacing between the lateral crystal planes observed during the first crystallization stage can be ascribed to the increase of internal stress associated with the contractive force emerging in the fiber. Once the temperature reaches 140 °C, the force reduces (see Figure 7), thus leading to the recovery of the cell parameters. As compared in Figure 9, the nonoriented PET sample shows a completely different feature in d spacing changes from that of the oriented

chains, but the two samples merge into a common equilibrium value at high temperatures.

Acknowledgment. X-ray diffraction was performed at the 4C1 beamline in the Pohang Accelerator Laboratory.

References and Notes

(1) Ward, I. M. *Adv. Polym. Sci.* **1985**, *70*, 1.
(2) Keller, A.; Lester, G. R.; Morgan, L. B.; Hartley, F. D.; Lord, E. W. *Philos. Trans. R. Soc. London* **1954**, A1, 247, 13.
(3) Zachmann, H. G.; Stuart, H. A. *Makromol. Chem.* **1981**, *181*, 1263.
(4) Zachmann, H. G.; Stuart, H. A. *Makromol. Chem.* **1960**, *41*, 131.
(5) Zaroulis, J. S.; Boyce, M. C. *Polymer* **1997**, *38*, 1303.
(6) Llana, P. G.; Boyce, M. C. *Polymer* **1999**, *40*, 6729.
(7) Bonart, R. *Kolloid-Z.* **1966**, *213*, 1.
(8) Bonart, R. *Kolloid-Z.* **1966**, *213*, 16.
(9) Bonart, R. *Kolloid-Z.* **1968**, *231*, 438.
(10) Asano, T.; Seto, T. *Polym. J.* **1973**, *5*, 72.
(11) Asano, T.; Francisco, J.; Baltá Calleja; Flores, A.; Tanikaki, M.; Mina, M. F.; Sawatari, C.; Itagaki, H.; Takahashi, H.; Hatta, I. *Polym. J.* **1999**, *40*, 6475.
(12) Yeh, G. S. Y.; Geil, P. H. *J. Macromol. Sci., Part B* **1967**, *1*, 235.
(13) Yeh, G. S. Y.; Geil, P. H. *J. Macromol. Sci., Part B* **1967**, *1*, 251.
(14) Murthy, N. S.; Correale, S. T.; Minor, H. *Macromolecules* **1991**, *24*, 1185.
(15) Gorlier, E.; Haudin, J. M.; Billon, N. *Polymer* **2001**, *42*, 9541.
(16) Mahendrasingam, A.; Martin, C.; Fuller, W.; Blundell, D. J.; Oldman, R. J.; Harvie, J. L.; Mackerron, D. H.; Riekel, C.; Engstrom, P. *Polymer* **1999**, *40*, 5553.
(17) Mahendrasingam, A.; Martin, C.; Fuller, W.; Blundell, D. J.; Oldman, R. J.; Mackerron, D. H.; Harvie, J. L.; Riekel, C. *Polymer* **2000**, *41*, 1217.
(18) Welsh, L.; Blundell, D. J.; Windle, A. H. *Macromolecules* **1998**, *31*, 7562.
(19) Shaofeng, R.; Wang, Z.; Burger, C.; Chu, B.; Hsiao, S. B. *Macromolecules* **2002**, *35*, 10102.
(20) Blundell, D. J.; Mahendrasingam, A.; Martin, C.; Fuller, W.; Mackerron, D. H.; Harvie, J. L.; Oldman, R. J.; Riekel, C. *Polymer* **2000**, *41*, 7793.
(21) Ward, I. M.; Hadley, D. W. *An Introduction to the Mechanical Properties of Solid Polymers*; John Wiley & Sons: New York, 1993; p 219.
(22) Ziabiki, A.; Kawai, H. *High-Speed Fiber Spinning, Science and Engineering Aspects*; John Wiley & Sons: New York, 1985; p 310.
(23) Auriemma, F.; Corradini, P.; De Rosa, C.; Guerra, G.; Petraccone, V.; Bianchi, R.; Di Dino, G. *Macromolecules* **1992**, *25*, 2490.
(24) Pereira, J. R. C.; Porter, R. S. *Polymer* **1984**, *25*, 877.
(25) Alfrey, T.; Mark, H. *J. Phys. Chem.* **1942**, *46*, 112.
(26) Bosley, D. E. *J. Polym. Sci., Part C* **1967**, *20*, 77.
(27) Mandelkern, L.; Roberts, D. E.; Diorio, A. F.; Posner, A. S. *J. Am. Chem. Soc.* **1959**, *81*, 4148.
(28) Grebowicz, J. S.; Brown, H.; Chuah, H.; Olvera, J. M.; Wasiak, A.; Sajkiewicz, A.; Ziabicki, A. *Polymer* **2001**, *42*, 7153.
(29) Atkinson, J. R.; Biddleston, F.; Hay, J. N. *Polymer* **2000**, *41*, 6965.
(30) Wu, G.; Yoshida, T.; Cuculo, J. A. *Polymer* **1997**, *38*, 1091.
(31) Wu, G.; Yoshida, T.; Cuculo, J. A. *Polymer* **1998**, *39*, 6473.
(32) Tadokoro, H.; Tatsuka, K.; Murahashi, S. *J. Polym. Sci.* **1962**, *59*, 413.
(33) Mahendrasingam, A.; Blundell, D. J.; Martin, C.; Fuller, W.; Mackerron, D. H.; Harvie, J. L.; Oldman, R. J.; Riekel, C. *Polymer* **2000**, *41*, 7803.
(34) Wakelyn, N. T. *J. Polym. Sci.* **1983**, *28*, 3599.
(35) Sun, T.; Zhang, A.; Li, F. M.; Porter, R. S. *Polymer* **1988**, *29*, 2115.
(36) Zhang, A. *Polymer* **1985**, *3*, 216.

MA034694I